

ARTICLE

The effect of length and inclination of carbon fiber reinforced polymer laminates on shear capacity of near-surface mounted retrofitted reinforced concrete beams

Mohammad Al-Zu'bi^{1,2} | Mizi Fan¹  | Yousef Al Rjoub²  |
Ahmed Ashteyat³  | Mazen J. Al-Kheetan^{4,5}  | Lorna Anguilano⁶

¹Department of Civil and Environmental Engineering, College of Engineering, Design and Physical Sciences, Brunel University London, Middlesex, UK

²Department of Civil Engineering, College of Engineering, Jordan University of Science and Technology, Irbid, Jordan

³Department of Civil Engineering, College of Engineering, The University of Jordan, Amman, Jordan

⁴Department of Civil and Environmental Engineering, College of Engineering, Mutah University, Karak, Jordan

⁵Materials Science and Energy Lab, MSEL, College of Engineering, Mutah University, Karak, Jordan

⁶Experimental Techniques Centre, College of Engineering, Design and Physical Sciences, Brunel University London, Uxbridge, Middlesex, UK

Correspondence

Mizi Fan, Department of Civil and Environmental Engineering, College of Engineering, Design and Physical Sciences, Brunel University London, Kingston Ln, Uxbridge, Middlesex, UK, UB8 3PH.

Email: mizi.fan@brunel.ac.uk

Funding information

Deanship of Research at Jordan University of Science and Technology, Grant/Award Number: 214/2016

Abstract

This study undertakes a comprehensive investigation of the shear behavior of reinforced concrete (RC) beams strengthened by near surface mounted (NSM) carbon fiber reinforced polymer (CFRP) laminates. Different strengthening configurations were employed by varying the length and inclination angle of the CFRP laminates. Results indicated that NSM-CFRP strengthening increased the load-carrying capacity, ductility, stiffness, and toughness from 8% to 41%, 9% to 78%, 24% to 159%, and 22% to 254%, respectively. Results also confirmed that as the CFRP laminate length decreases, the efficacy of the strengthening process increases, where the load-carrying capacity, ductility, stiffness, and toughness improved from 8% to 19%, 10% to 21%, 8% to 68%, and 26% to 119%, respectively. Also, the comparative results revealed that specimens strengthened with 45°-inclined CFRP laminates versus those strengthened with vertical laminates had higher load-carrying capacity (2%–10%), ductility (1%–35%), stiffness (24%–40%), and toughness (13%–32%). Two analytical formulations to predict the contribution of the possible distinct NSM-CFRP shear strengthening configurations for the shear resistance of RC beams were considered. Results indicated an agreement between the experimental and the analytical results for both formulas, where the average values for the safety factor, k , ($k = V_t^{\text{ana}}/V_t^{\text{exp}}$) were 0.80 and 0.73, with corresponding values of standard deviation of 0.195 and 0.125, respectively.

KEYWORDS

analytical results, CFRP laminates, experimental results, NSM technique, RC beams, shear strengthening

Discussion on this paper must be submitted within two months of the print publication. The discussion will then be published in print, along with the authors' closure, if any, approximately nine months after the print publication.

This is an open access article under the terms of the Creative Commons Attribution License, which permits use, distribution and reproduction in any medium, provided the original work is properly cited.

© 2021 The Authors. *Structural Concrete* published by John Wiley & Sons Ltd on behalf of International Federation for Structural Concrete.

1 | INTRODUCTION

Fiber reinforced polymer (FRP) materials have been used for structural retrofitting since the 1990s. This may be because of continuing reductions in the cost of these materials and their many advantages compared with conventional strengthening materials, such as steel, wood, and concrete. These advantages include their high strength-to-weight ratio (i.e., high modulus of elasticity and high tensile strength), high durability (noncorrosive), low thermal conductivity, electromagnetic neutrality, ease of handling, rapid execution with less labor, reduced mechanical fixing, lower installation cost and reduced maintenance cost, excellent malleability, and unlimited availability in size, geometry, and dimensions. Therefore, their use for retrofitting purposes has gained considerable popularity worldwide and can produce confident strengthening and repairing systems for existing concrete structures.¹⁻⁵ The externally bonded reinforcement (EBR) strengthening system is the most widespread system for strengthening/retrofitting reinforced concrete (RC) beams. However, the technique suffers from premature debonding of FRP composites from concrete substrate because they are susceptible to the risk of fire and physical damage and vandalism as a result of a collision during the process of stress transmission and humidity effect for being open to atmosphere. Therefore, the EBR technique cannot develop full FRP's strength, as the full capacity of FRP reinforcements cannot be utilized.⁶⁻¹¹ The previously mentioned disadvantages of EBR-FRP system (i.e., debonding failure) have led the researchers to adopt another strengthening/retrofitting system to provide the retrofitted concrete beams better performance under harsh conditions. Near surface mounted (NSM) system was found to be the most appropriate alternative.

The concept of NSM method was invented from the repair of concrete structures in the 1940s in Europe utilizing insertion steel rebars into slits cut into the surface of the concrete structures using cement mortar.¹² NSM-FRP technique is based on embedding FRP materials, of circular, square, or rectangular cross-section, into grooves cut onto the surface of the beam and filled with an appropriate adhesive, such as epoxy paste or cement grout.^{13,14}

It was also found that NSM technique has many advantages over EBR counterpart; for example, it requires no surface preparation work and requires minimal installation time after cutting the thin slit. As the NSM reinforcement is protected by the concrete cover, this would protect the embedded FRP reinforcement against harm resulting from vandalism, mechanical damage, fire, harsh environment, and aging effects. Therefore, NSM-FRP system tends to deliver greater bond condition than that of EBR-FRP materials, and they are

consequently less prone to debonding from the concrete substrate. Moreover, the appearance/aesthetic of the strengthened element is practically unaffected by the strengthening intervention.^{13,15,16}

Moreover, many research studies have found that the NSM-FRP-strengthened beams have shown better performance, in terms of shear capacity and maximum strain, than those strengthened with EBR-FRP materials. For instance, Dias and Barros^{13,17} concluded that the NSM technique is much more efficient than EBR, since it provides a larger increase in maximum load, load-carrying capacity after shear crack formation, and maximum strains in the CFRP materials. Moreover, NSM is simpler and faster to apply than EBR. Rizzo and De Leronzi,¹⁴ results exhibited that the increase in shear capacity was about 16% for the beam strengthened with externally bonded (EB) U-wrapped laminate and ranged between 22% and 44% for the beams strengthened with NSM reinforcement. It was also verified that the use of NSM reinforcement was more effective in terms of exploitation of the FRP tensile strength due to early debonding of the EB laminate. The EB-FRP-strengthened beam failed by debonding the CFRP laminate, while separation of the side concrete covers of the internal steel stirrups was the governing mode of failure for the NSM-FRP-strengthened specimens. Dias and Barros¹⁸ found that the NSM-CFRP technique was more efficient than the EBR-CFRP counterpart. This efficacy was not only in terms of the beam load-carrying capacity, but also in terms of the deformation capacity at beam failure. The beams strengthened by EBR and NSM techniques showed an average increase of 54% and 83% load-carrying capacity, respectively, compared with the unreinforced beams. The same observations were recorded by Barros and Dias,¹⁹ but they also found that the beams strengthened by EBR and NSM techniques showed increments in deflection of 77% and 307%, respectively, compared with the unreinforced beams, indicating that the efficacy of the NSM was more pronounced in terms of deformability index. The failure modes of the beams strengthened by the NSM technique were not as brittle as the ones observed in the beams strengthened by the EBR technique. It was also confirmed that the NSM shear strengthening technique was easier and faster to apply than the EBR technique. From the obtained results of the test conducted by Dias and Barros,²⁰ it could be concluded that NSM technique was more effective than EBR, because NSM provided a higher increase, not only in terms of beam's load-carrying capacity but also in terms of stiffness after shear crack formation. The values of load-carrying capacity and stiffness after the shear crack formation of the EBR beams were 34% and 59% of the values obtained in the NSM beams. NSM also provided higher values of maximum strains measured in the CFRP. When compared with the

homologous conventionally shear reinforced beam (reference beam), the NSM-shear strengthened beams presented 90% of the maximum load of the reference beam and higher stiffness, mainly after shear crack initiation. In comparison, the EBR-shear strengthened beam had a maximum load that was 79% of the maximum load of the reference beam and similar stiffness up to the initiation of the debonding process of the wet lay-up CFRP strips of the sheet.

Other research studies have confirmed the efficiency of using NSM-FRP materials for the shear strengthening of RC beams. For example, De Leronzis and Nanni²¹ reported that the use of NSM-FRP rods is an effective technique to enhance the shear capacity of RC beams. Dias and Barros²² found that NSM technique with CFRP laminates provided a significant contribution to the shear resistance of RC T-beams. Mofidi et al.²³ reported that the near-surface mounted method greatly enhanced the overall behavior of RC beams. It was found in another study that the CFRP shear strengthening configurations provided an increase not only in terms of maximum load but also in terms of load-carrying capacity after shear crack formation.⁴ Further investigation showed that the NSM-CFRP shear strengthening systems significantly increased the shear resistance of concrete beams.¹⁸ It was indicated by other research that all CFRP reinforcement applications increased the strength and behavior of the shear deficient specimens in a different manner.²⁴ The NSM-CFRP rods effectively strengthen RC beams in shear, as shown in.¹⁴ The load-carrying capacity of reinforced concrete beams can be significantly increased using the NSM-CFRP shear strengthening systems.¹⁹

It is noteworthy that the shear strengthening of RC beams with NSM-FRP materials is affected by several parameters, such as the length and inclination of the NSM-FRP reinforcement bonded to the concrete substrate. While research studies have investigated the effect of inclination and concluded that the NSM-CFRP laminates inclined at 45° with the beam axis were more effective in terms of shear capacity and stiffness of the strengthened beams than the vertical laminates (positioned at 90°),^{3,14,17–19,21} the influence of the bonded length of NSM-CFRP laminates has not been studied yet. This study is dedicated to investigating the combined effect of the length and inclination of NSM-CFRP laminates on the shear strengthening of RC beams in terms of load-carrying capacity, maximum deflection, and stiffness and toughness through experimental tests. Analytical formulas are also used to validate the experimental results.

Moreover, it was reported that the efficiency of NSM-FRP strengthening system is related to the groove size.³² It was also confirmed that increasing the groove width would increase the resistance to concrete split failure. Another investigation showed that groove dimensions of

5 mm width by 25 mm could accommodate CFRP laminates with a nominal width of 50 mm and a total thickness of 1.2 mm, which are adequate to prevent splitting of the epoxy cover.³³ Furthermore, it was observed that increasing the groove size would lead to a higher bond strength, ultimate load, and fracture energy of the NSM joints, and offer a higher resistance to splitting of the epoxy cover, because that reduces the state of stress in the concrete adjacent to the groove sides and hence delays its cracking phenomena.^{34–38} However, it was found by Soliman et al.³⁹ that increasing the groove size for specimens with epoxy adhesive did not have a significant influence on the failure load, but it decreased failure load for specimens with cement adhesive. Also, Gómez et al.⁴⁰ found that the failure loads and the bond strength were slightly higher for specimens with narrower grooves. The failure modes were changed from FRP–adhesive interface failure in specimens with the wider grooves to failure in resin–concrete interface in case of the narrower grooves. Al-Mahmoud et al.⁴¹ noticed that the ultimate pull-out loads were significantly lower in the case of rectangular grooves (20 × 50 mm) than in square grooves (20 × 20 mm and 30 × 30 mm).

2 | EXPERIMENTAL PROGRAM

2.1 | Test specimens

A total of seven simply supported RC beams with dimensions of 15 cm × 25 cm × 130 cm were constructed. All beams had the same flexural and shear reinforcements, designed to ensure that un-strengthened and shear-strengthened beams would all fail in shear. The steel tension and compression reinforcement consisted of three 14 mm-diameter and two 10 mm-diameter rebars, respectively, with a clear concrete cover for steel reinforcements of 2.5 cm. The shear reinforcement included 6 mm-diameter closed double-legged stirrups at a spacing of 20 cm. General layout and reinforcement details of the test specimens are shown in Figure 1. It must be noted that the beams' shear span-to-effective depth (a/d) ratio is about 2.14, which is not considered very low. The a/d ratio has a more significant influence on the shear strength of beams without shear reinforcement. Using concrete with moderate compressive strength can minimize the arch effect. So that the arch effect on the results could be ignored.

Six beams were strengthened with carbon fiber reinforced polymer (CFRP) laminates bonded to the beam web on both sides, while one beam was un-strengthened to work as a control. The test variables are:

- length of the NSM-CFRP laminates. Three different lengths were considered: laminates lying on the full-

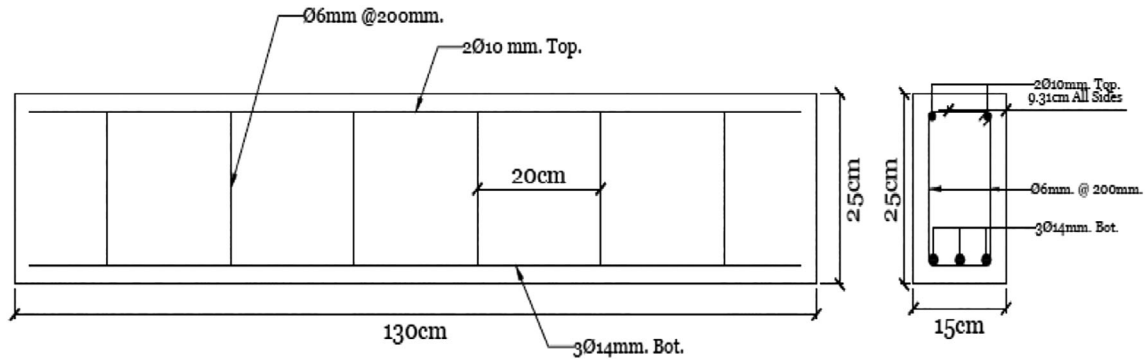


FIGURE 1 Dimensions and reinforcement details of the test specimens

TABLE 1 Retrofitting design

Specimen	NSM-CFRP laminates inclination angle	Trimming of NSM-CFRP laminates (cm)	Length of NSM-CFRP laminates (cm)
FD-90	90	0	25
T ₃ -90	90	3	19
T ₅ -90	90	5	15
FD-45	45	0	25
T ₃ -45	45	3	19
T ₅ -45	45	5	15

beam depth, and laminates trimmed by 3 and 5 cm from both ends. It must be noted that only 3 and 5 cm were chosen as a representative, while it is envisaged that other length varieties could be studied in future;

- the inclination of the NSM-CFRP laminates with respect to the axis of the beam. Two different inclinations were selected: 90° (vertical reinforcement) and 45°.

Table 1 illustrates the test program. The control beam is indicated by CB. The codes used for the strengthened beams are characterized by two initial letters indicating the trimming value of the NSM-CFRP laminates (FD for the laminates lying on the full-beam depth, T₃ and T₅ for the laminates trimmed by 3 and 5 cm, respectively), followed by two digits indicating the inclination angle of the CFRP laminates (90° or 45°). Also, Figure 2 shows the NSM-CFRP strengthening configuration.

2.2 | Material properties

In this study, concrete with 28-day average compressive strength of 32.2 MPa, determined on standard (100 mm diameter × 200 mm height) concrete cylinders with a slump of 120 mm was prepared. Ordinary Portland cement

(type I) crushed coarse limestone aggregates with a maximum size of 12.5 mm, and a 20/80 mixture of silica sand and fine limestone was used to prepare the concrete mix following the ACI 318-14 mix design procedure. The water-to-cement ratio (w/c) was maintained at 0.47. A commercially available super-plasticizer at ratios of 0.75%, 1.00%, and 1.25% by weight of water was used. Steel reinforcing rebars (diameters of 14 and 10 mm, average yield stress of 464 and 424 MPa, respectively) were used as longitudinal reinforcement. Steel stirrups (diameter 6 mm, yield stress of 381 MPa) were used as transverse reinforcement. Commercially available CFRP laminates (Sika CarboDur S1.525) with 15 mm width and 2.5 mm thickness were used. Their tensile strength and elastic modulus, as provided by the manufacturer, are 2.8 and 165 GPa, respectively. A two-component epoxy resin (Sikadur-30 LP), with tensile strength and tensile elastic modulus of 14 MPa and 10 GPa, respectively, as provided by the manufacturer, was used in this study.

It is noteworthy that the arrangement of CFRP laminates (i.e., spacing) was adopted in our study from one of those that have been reported for the CFRP laminates, as the spacing between CFRP laminates was not the focus of this study. The coverage of shear zones (between loads and supports from both sides) with CFRP laminates was critical to be investigated regardless of spacing. Therefore, one of the most commonly used spacing, 8 cm was used in this study.

2.3 | Specimen preparation and test setup

Test specimens were cast into horizontally positioned wooden molds. Twenty-four hours after casting, the beams were de-molded and wet cured for 28 days. After that, the retrofitting process was applied according to the following procedure: (a) using a diamond cutter, grooves (of about 8 mm in width and 22.5 mm in depth) were

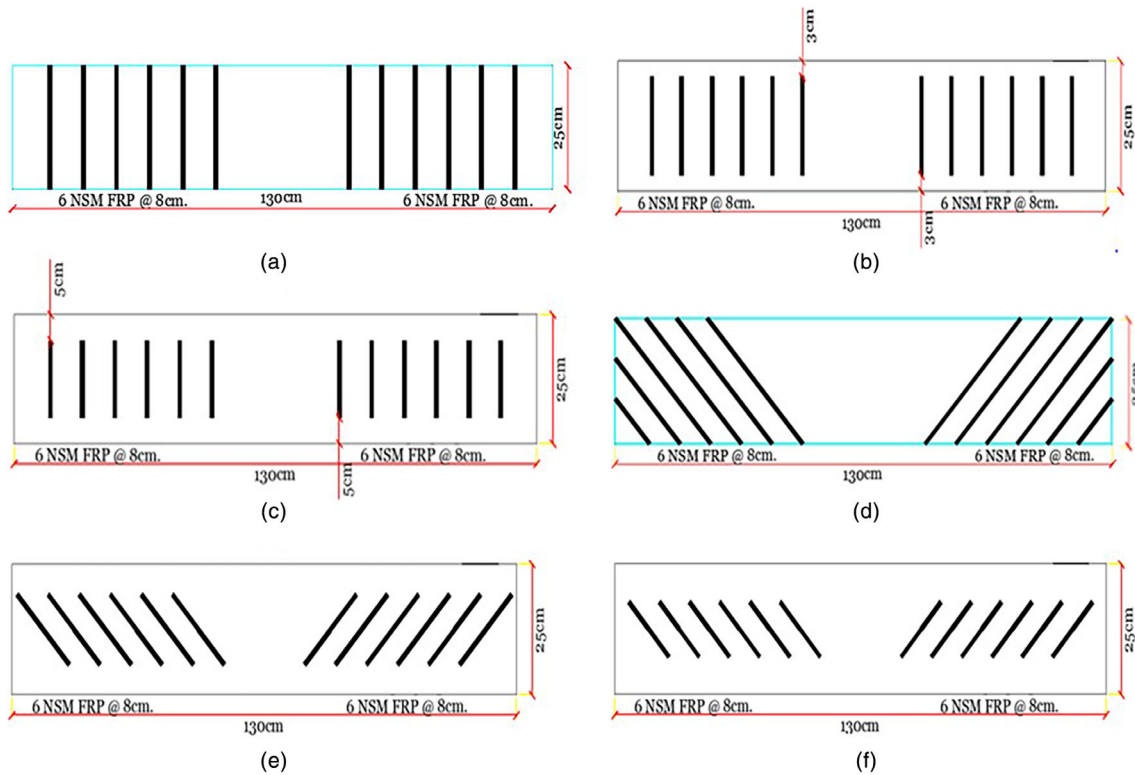


FIGURE 2 NSM-CFRP strengthening configuration (a) FD-90, (b) T_3 -90, (c) T_5 -90, (d) FD-45, (e) T_3 -45, and (f) T_5 -45

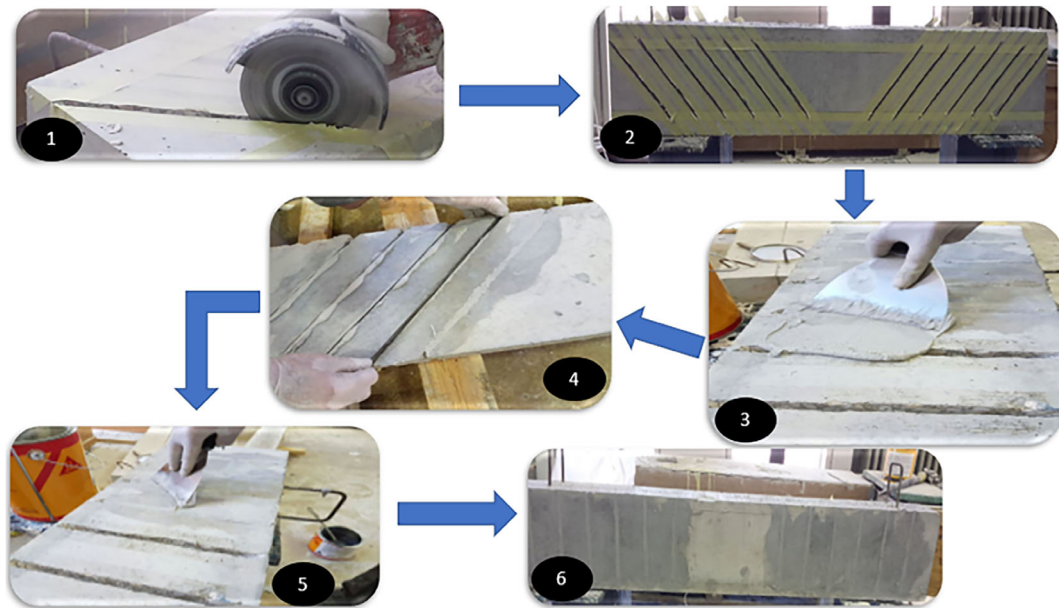


FIGURE 3 NSM-CFRP strengthening process

opened into the concrete cover of the lateral faces of the beam web; (b) the grooves were cleaned by compressed air; (c) the CFRP laminates were cut to the desired length; (d) epoxy adhesive pastes were obtained by mixing component A and component B in a 3:1 weight ratio; (e) the grooves were filled halfway with the

adhesive; (f) a layer of adhesive was applied on the faces of the strips; and (g) the strips were inserted into the grooves and excess removed (see Figure 3). It's noteworthy that the groove size considered in this study was taken according to ACI 440.2 R-08,²⁸ in which a minimum groove size of $3.0a_b \times 1.5b_b$, as shown in Figure 4,

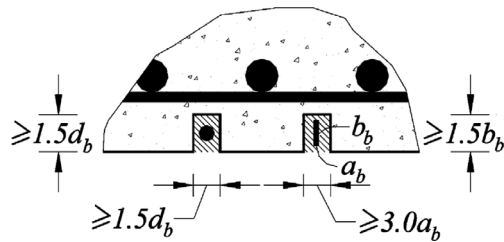


FIGURE 4 Minimum dimensions of grooves²⁸

is suggested, where, a_b is the smallest bar dimension. The same groove size, mentioned above, was considered for all strengthened specimens, so its effect on the beam capacity was not investigated.

All beams were tested under four-point loading using a hydraulic testing machine with a capacity of 370 kN and a load rate of 0.25–0.50 kN/s, which was appropriately manually changed for testing. The vertical displacement at the point of the load application was measured using linear variable displacement transducers (LVDTs) placed at the mid-span of the beams. The load was gradually increased using displacement control, and both shear and flexural cracks were observed on the concrete surface until failure. The load and displacement values were then recorded using a data acquisition system, as shown in Figure 5.

3 | RESULTS AND DISCUSSION

3.1 | Failure loads and maximum deflections

The failure loads of the tested beams and their maximum mid-span deflections are provided in Table 2. The strengthened beams experienced significant increases in load-carrying capacity and deflection compared with the control beam.

Table 3 shows the effect of varying length and inclination of CFRP laminates on the maximum loads and deflections of strengthened specimens. As for the effect of length of CFRP laminates, the beam T₃-90 exhibited an increase of about 8% and 10% in the maximum load and deflection, respectively, compared with the beam FD-90. The beam T₅-90 showed an increment in the maximum load and deflection of about 19% and 21% compared with the beam FD-90, and about 11% and 10%, respectively, compared with the beam T₃-90. It can be noted that the rate of increment in maximum loads and deflections increases with decreasing the length of CFRP laminates.

As for the effect of CFRP inclination angle, the beam FD-45 showed an increment of about 2% and 1% in the maximum load and deflection respectively, compared

with beam FD-90, while beam T₃-45 exhibited an increase of about 5% and 4% compared with beam T₃-90, while beam T₅-45 showed an increment of about 10% and 35% respectively, compared with beam T₅-90. It can be observed that strip inclination also results in an improvement in the shear resistance, as evidenced by CFRP strips becoming normalized to the shear crack direction, preventing the propagation of shear cracks.

In summary, the results showed that the maximum loads and deflections of the strengthened specimens increased as the length of CFRP laminates decreased and the CFRP inclination angle increased. It can also be noticed that changing CFRP length had a more significant effect on the maximum loads and deflections than varying the inclination angles, except in the case of the beam strengthened with 5 cm-trimmed laminates (T₅-45). This may confirm that using shorter CFRP laminates may result in a more effective strengthening process.

3.2 | Failure modes

Figure 6a–g illustrates the failure modes of all tested specimens. It is clear from Figure 6a that specimen CB failed due to shear cracks, and concrete crushing which caused a peeling-off of the side concrete cover and delamination of the top and bottom concrete covers. This failure mode appeared because the beam is minimally shear-reinforced while it was properly reinforced in flexure. Many shear cracks started appearing at 42 kN and continued until failure. However, it is noticed from Figure 6b that shear failure governed the failure mode of specimen FD-90, and concrete crushing, which resulted in delamination of the bottom concrete cover. A smaller number of shear cracks appeared compared with the control specimen. This means that the strengthening could control crack propagation. However, the first crack was at 39 kN, which is a bit smaller than that shown in the control beam. This was attributed to the grooves continuing to the end of the specimen, which resulted in the formation of weak points by inducing stress concentration at those zones. The shear failure crack has crossed two CFRP laminates.

On the other hand, a major shear crack and concrete crushing leading to delamination of the bottom concrete cover and peeling-off of the side concrete cover caused the failure of specimen T₃-90 (Figure 6c). The minor shear cracks were noted to be less than those that had appeared in the control specimen. However, the first crack appeared at 31 kN, which is also smaller than that appeared in the control beam. This means that, although the grooves in this strengthening configuration did not continue to the beam end, they failed to control the shear cracks. There are three CFRP laminates that the shear

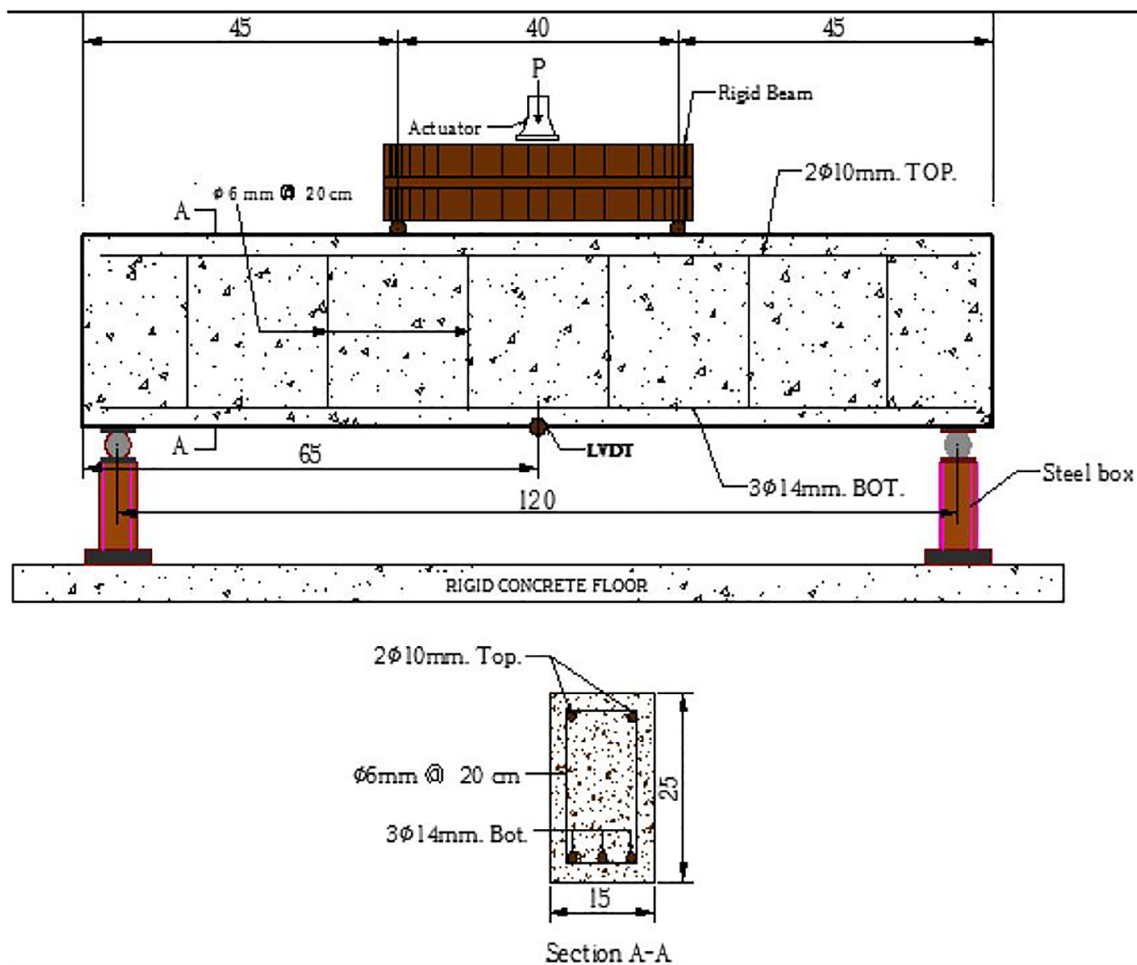


FIGURE 5 Illustrative sketch of the test setup (dimensions are in cm)

TABLE 2 Maximum failure loads and deflections of specimens

Specimen	Load at first crack (kN)	Ultimate load (kN)	Failure mode	Maximum deflection (mm)	Load strengthening ratio (%)	Ductility improving ratio (%)
CB	42	192	Shear and CC ^a	6.89	–	–
FD-90	39	207	Shear and CC	7.53	7.81	9.29
T ₃ -90	31	223	Shear and CC	8.30	16.15	20.46
T ₅ -90	51	247	Shear and CC	9.10	28.65	32.08
FD-45	43	211	Flexure and CC	7.64	9.90	10.89
T ₃ -45	50	234	Shear and CC	8.60	21.88	24.82
T ₅ -45	50	271	Shear and CC	12.30	41.15	78.52

^aCC, concrete crushing.

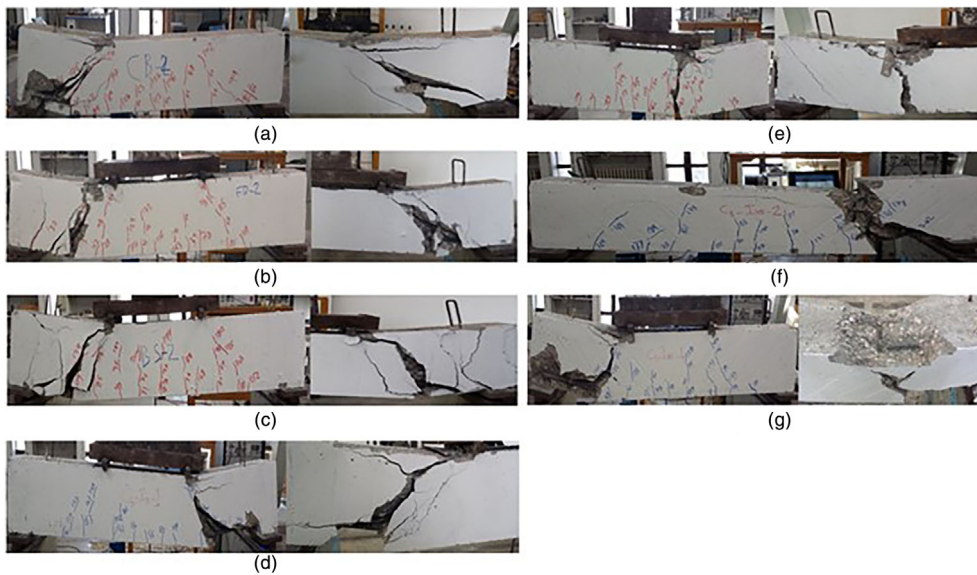
failure crack has crossed. The same failure mode that appeared in beam T₃-90 was the dominant in specimen T₅-90, as shown in Figure 6d, although the first crack appeared at 51 kN. This means that the installation of the CFRP strips at 5 cm from the beam end could delay crack formation. This might be attributed to the fact that the

crack faced a non-grooved strong surface, which was able to prevent the premature crack formation that had happened in the previous specimens. The shear crack at failure has intercepted only two CFRP laminates.

Interestingly, specimen FD-45 failed due to flexural cracks and concrete crushing, which resulted in peeling-

TABLE 3 The effect of length and inclination of CFRP laminates on the performance of strengthened beams

The effect of CFRP laminates length				
Specimens	Load strengthening ratio (%)	Ductility improving ratio (%)	Increasing in stiffness (%)	Increasing in toughness (%)
T ₃ -90 vs. FD-90	7.73	10.23	8.34	25.82
T ₅ -90 vs. FD-90	19.32	20.85	67.74	119.16
T ₅ -90 vs. T ₃ -90	10.76	9.64	54.83	74.19
The effect of CFRP laminates inclination				
FD-45 vs. FD-90	1.93	1.46	30.76	12.63
T ₃ -45 vs. T ₃ -90	4.93	3.61	39.63	22.88
T ₅ -45 vs. T ₅ -90	9.72	35.16	24.13	32.41


FIGURE 6 Failure modes: (a) CB, (b) FD-90, (c) T₃-90, (d) T₅-90, (e) FD-45, (f) T₃-45, and (g) T₅-45

off of the side concrete cover (Figure 6e). A few numbers of shear cracks formed. This could be interpreted as the installation of CFRP laminates normal to the shear cracks in this configuration could prevent their propagation. The first crack appeared at 43 kN, which is almost the same as in the control specimen. The specimen failed at a lower load compared with those failed due to shear cracks. This is because the formation of shear cracks in this strengthening configuration could be prevented. Thus, some flexural cracks in the zone of the maximum moment were directly formed and propagated, causing a quick failure at a low load. While in the case of beams that failed in shear, the shear cracks were able to form and propagate, and such a shear crack forms and propagates until it faces a CFRP laminate, which stops it; afterward, more cracks formed until failure. Thus, that took more time and therefore led those beams to fail at higher loads.

On the other hand, in specimen T₃-45 (Figure 6f) it is observed that shear cracks and concrete crushing caused

the side concrete cover to peel-off and delamination of the top and bottom concrete covers led to failure, in addition to CFRP laminate deterioration. Moreover, the number of shear cracks formed and propagated was much smaller than those that had appeared in the control beam (Figure 6f). The beam showed an ability to delay crack formation in that the first crack appeared at 50 kN. The mode of failure of this beam shows that the shear failure crack has crossed all CFRP laminates.

Specimen T₅-45 showed a similar failure mode to specimen T₃-45 with the same load at the first crack but with no CFRP laminate impairment, as shown in Figure 6g. However, this specimen showed a higher ultimate load than specimen T₃-45. This may refer to the location of grooves that were in a farther distance from the specimen's end, which led the crack to face a non-grooved firm surface that was able to prevent premature crack formation, giving the specimen more resistance to shear crack propagation, as in the case of the beam T₅-90. The shear crack at failure has intercepted five CFRP laminates.

FIGURE 7 Load-deflection relations

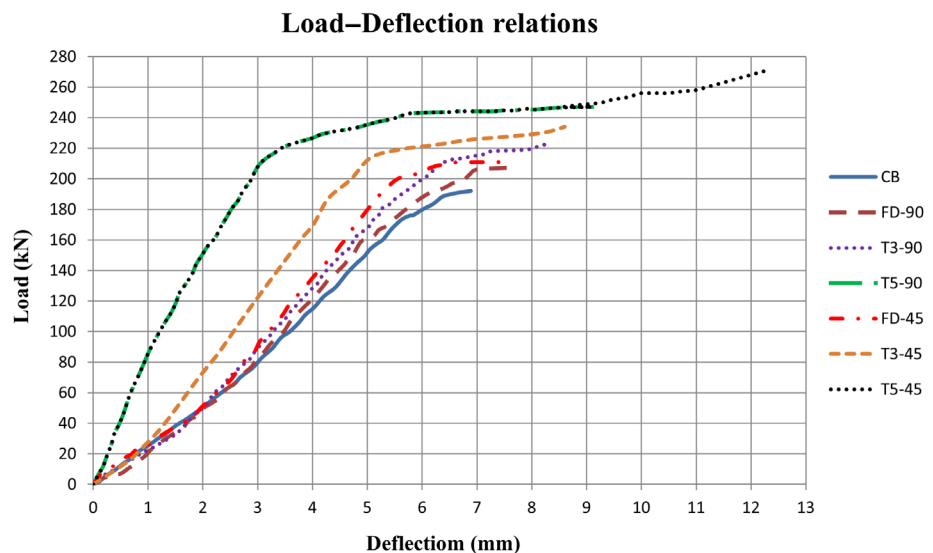


Figure 7 shows the load–deflection relations for all tested specimens. The curves start linear until cracks (i.e., shear cracks in the beams failed in shear and flexural cracks in the beam failed in flexure) appear, then the non-linearity region continues until failure. It is clear that all strengthened specimens showed higher values of maximum deflection and failure load than the control specimen. In addition, the specimens strengthened with shorter-length CFRP strips offered higher maximum deflection and failure load values. A slighter change of maximum deflection and failure load was observed for specimens strengthened with inclined strips.

3.3 | Calculation of stiffness and toughness

The stiffness and toughness values of all specimens and the increasing percentages compared with the control specimens are provided in Table 4.

3.3.1 | Stiffness calculation

The stiffness (k) is defined as the extent to which the element can resist deformation or deflection under the action of an applied force. The stiffness of such a specimen equals the slope of the elastic portion of its load–deflection curve. As shown in Table 4, all strengthened specimens exhibited higher values than the control specimen. The reason beyond that is that the NSM-CFRP strengthening provides the specimens with more ductility, because it delayed the formation of shear or flexural cracks (depending on the beam's failure mode), as discussed in Section 3.1, which makes

them able to resist more deformation before failure, compared with the control beam. Moreover, it was found that as the length of CFRP laminates decreases and their inclination angle increases, the stiffness increases, as shown in Table 3. These results support what was found regarding the ultimate loads and maximum deflections.

3.3.2 | Toughness calculation

Toughness is referred as the capability of the material to absorb energy and deform plastically without any fracture. Mathematically, toughness relates to the area under the load–deflection curve. There are several methods to find the area, of which this study used the integration approach, in which, the toughness is calculated through calculating the integration of the function of the best-fit line of the load–deflection curve of such a specimen along the x-axis, from 0 to its maximum deflection value shown in Table 2. For example, if we take specimen FD-90, the area under its curve equals the integration of the function, as follows:

$$\text{Toughness} = \int_0^{7.53} (0.0053x^6 - 0.0946x^5 + 0.5236x^4 - 1.3405x^3 + 5.3053x^2 + 15.955x) = 830.26 \text{ J}$$

Table 4 illustrates that all strengthened specimens showed higher toughness values than the control specimen. This is because the strengthening with NSM-CFRP laminates makes the specimens more ductile. Therefore, it resisted both shear and flexural cracks propagation, as discussed in Section 3.1, which provides them with more

TABLE 4 Stiffness and toughness values and strengthening ratios

Specimen	Stiffness (kN/mm)	Increasing in stiffness (%)	Toughness (J)	Increasing in toughness (%)
CB	26.19	–	681.22	–
FD-90	32.61	24.51	830.26	21.89
T ₃ -90	35.33	34.90	1044.60	53.34
T ₅ -90	54.70	108.86	1819.57	167.10
FD-45	42.64	62.81	935.16	37.28
T ₃ -45	49.33	88.35	1283.64	88.43
T ₅ -45	67.90	159.26	2409.24	253.67

extended periods to absorb more energy before fracture if they are compared with the control beam. Like what happened regarding stiffness, it was also found that toughness increase with decreasing the CFRP laminates length and increasing their inclination angles, as shown in Table 3. These results agree with what was found regarding the ultimate loads and maximum deflections, as shown in Table 2.

The results obtained from the experimental tests in terms of the effect of inclination of CFRP laminates are in remarkable agreement with those existing in the literature.^{3,14,17–19,21} Where it was found herein that the inclined laminates provide a more efficient strengthening, in terms of maximum loads and deflections, stiffness, and toughness, than vertical laminates. This is in agreement with the literature regarding the better performance of specimens strengthened with inclined laminates compared with those with vertical laminates. As for the bonded length of CFRP laminates, there are no studies, to date, that have investigated the effect of this factor.

4 | ANALYTICAL INVESTIGATION

According to ACI 318-05,²⁷ the design of cross-sections subject to shear shall be based on Equation (1):

$$\phi V_n \geq V_u \quad (1)$$

where, V_u is the factored shear force at the section considered and V_n is nominal shear strength, the strength reduction factor $\phi = 0.85$. The approach used to calculate the nominal shear capacity of a member strengthened using NSM bars is like that used in ACI 440.2 R-08²⁸ for the case of externally bonded FRP laminates. Equation (2) is applicable for NSM systems. An additional reduction factor $\psi_f = 0.85$ is applied to the contribution of NSM-CFRP reinforcement to the shear strength of the member.

$$\phi V_n = \phi (V_c + V_s + \psi_f V_f) \quad (2)$$

where, V_c is the shear contribution of the concrete, which is calculated using Equation (3):

$$V_c = \frac{\sqrt{f'c} \times b_w \times d}{6} \quad (3)$$

where, $f'c$ is the concrete compressive strength; b_w is the width of concrete section; and d is the effective depth of concrete section.

V_s is the shear contribution of the steel stirrups, which is calculated using Equation (4):

$$V_s = \frac{A_v \times f_{yw} \times d}{S} \quad (4)$$

where, A_v is the cross-sectional area of steel stirrups; f_{yw} is the yield stress of steel stirrups; d is the effective depth of concrete section; and S is the spacing of steel stirrups.

To compute the contribution of NSM-FRP reinforcement to the shear capacity of RC beams (V_f), several analytical formulas have been proposed in the literature.^{4,21,25,26,29} The formulas proposed by Dias and Barros⁴ and Nanni et al.²⁹ are used herein to compute V_f , as follows.

4.1 | Formulas by Dias and Barros

Equation (5)⁴ is used to compute the contribution of CFRP laminates to the shear capacity of RC beams:

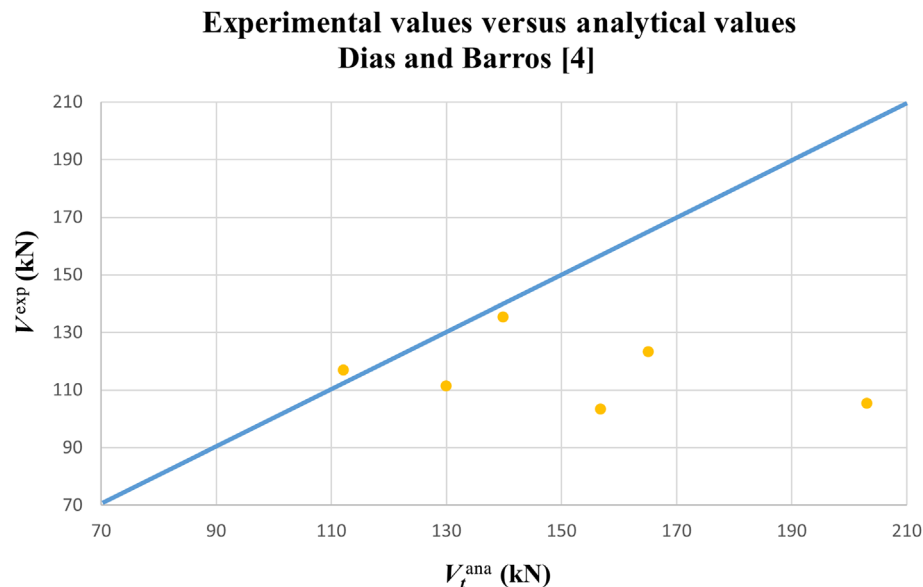
$$V_f = h_w \times \frac{A_{fv}}{S_f} \times \mathcal{E}_{fe} \times E_f \times (\cot \alpha + \cot \theta_f) \times \sin \theta_f \quad (5)$$

where, h_w is the web depth of the beam (equal to the length of vertical laminates); A_{fv} is the cross-sectional area of a FRP laminate; \mathcal{E}_{fe} is the effective strain of FRP

TABLE 5 Comparison between the experimental and analytical values

Specimen	V_t^{exp} (kN)	Dias and Barros ⁴		Nanni et al. ²⁹	
		V_t^{ana} (kN)	k ($V_t^{\text{exp}}/V_t^{\text{ana}}$)	V_t^{ana} (kN)	k ($V_t^{\text{exp}}/V_t^{\text{ana}}$)
FD-90	103.5	156.75	0.66	130.21	0.79
T ₃ -90	111.5	129.93	0.86	168.85	0.66
T ₅ -90	117.0	112.05	1.04	130.21	0.90
FD-45	105.5	203.04	0.52	52.93	-
T ₃ -45	123.5	165.06	0.75	216.87	0.57
T ₅ -45	135.5	139.83	0.97	189.55	0.71

FIGURE 8 Comparison between the experimental and analytical values, Dias and Barros⁴



laminates; E_f is the elastic modulus of FRP laminates; α is the orientation of the shear failure crack; θ_f is the inclination of the FRP laminates with respect to the beam axis; and s_f is the spacing of laminates.

The effective strain threshold (\mathcal{E}_{fe}) of 0.004 was suggested by Khalifa et al.³⁰ to maintain the shear integrity of the concrete and to avoid large shear cracks that could compromise the aggregate interlock mechanism. Also, the slope of the shear crack (α) was assumed to be at 45° . The values of h_w were 25 cm for beams FD-90 and FD-45, 19 cm for beams T₃-90 and T₃-45, and 15 cm for beams T₅-90 and T₅-45.

The experimental values (V_t^{exp}) and the analytical values (V_t^{ana}), and the safety factor, k ($k = V_t^{\text{exp}}/V_t^{\text{ana}}$), are provided in Table 5. Figure 8 also shows a comparison between V_t^{exp} and V_t^{ana} .

It is noteworthy that V_t^{exp} and V_t^{ana} represent, respectively, ϕV_n and V_u in Equation (1). According to Equation (1), for safety purposes, ϕV_n should be more than or equal V_u , or the ratio $\phi V_n/V_u$ should be more than 1. Therefore, to make sure the safety condition is met, the factor, k , was used. It was noticed that about 83% (5 out

of 6) of the specimens have k values below the unity, as shown in Table 5. Figure 8 also shows that these specimens are in the unsafe zone (below the diagonal line). In contrast, the beam T₅-90 presented a k value above the unity ($k = 1.04$). This is due to two main reasons, the first reason is the highest load at the first crack (51 kN) appeared in this specimen among all specimens. The shortest length of NSM-CFRP strips among those specimens with the same NSM-CFRP laminates inclination angle (90°) also contributed to achieve that high failure load (247 kN), which led to a high value of V_t^{exp} . The second reason is the relative low value of V_f (Equation (5)). This was due the low values of h_w (15 cm) and $\cot\theta_f$ (0) together. Therefore, the quotient ($V_t^{\text{exp}}/V_t^{\text{ana}}$) was the largest among all specimens.

The average k value was 0.80, and the corresponding standard deviation value was 0.195. The standard deviation of 0.195 for such a small number of samples is considered a bit high. It is because of the difference of V_f values due to using different values of h_w and θ_f in Equation (5), while the rest terms are constant for all specimens.

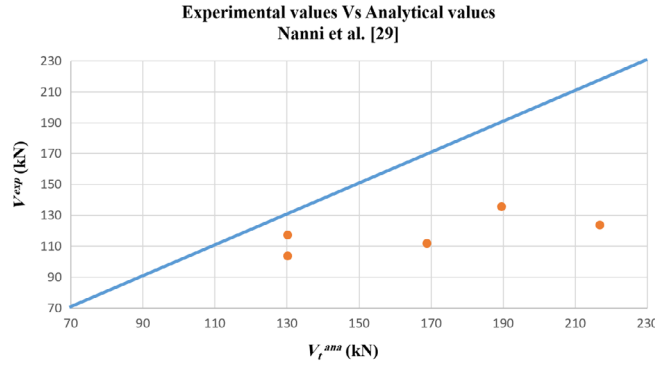


FIGURE 9 Comparison between the experimental and analytical values, Nanni et al.²⁹

4.2 | Formulas by Nanni et al.

The approach adopted by Nanni et al.²⁹ to calculate the nominal shear capacity of a member strengthened using NSM-FRP bars is a bit different from that considered by Dias and Barros,⁴ in which they used the equation provided by ACI 440.2R-02³¹ for the case of externally bonded FRP laminates (Equation (6)), assuming that it applies to NSM-FRP systems.

$$V_n = V_c + V_s + V_f \quad (6)$$

where, V_c is the nominal shear strength provided by concrete; V_s is the nominal shear strength provided by steel reinforcement; V_f is the nominal shear strength provided by FRP reinforcement; and V_n is the nominal shear strength at section.

The shear strength provided by the NSM-FRP reinforcement applied symmetrically on both sides of the girder web can be determined by calculating the force resulting from the tensile stress in the FRP bars across the assumed crack, and it is expressed for rectangular bars by Equation (7):

$$V_f = 4(a + b)\tau_b L_{tot} \quad (7)$$

where, a is the smaller dimension of a rectangular FRP bar; b is the larger dimension of a rectangular FRP bar; and τ_b is the average bond stress of the bars crossed by a shear crack.

A conservative value of $\tau_b = 6.9$ MPa (1.0 ksi) can be used when using an epoxy-based resin in a groove size at least 1.5 times the bar diameter.

L_{tot} can be expressed as:

$$L_{tot} = \sum_i L_i$$

where, L_i represents the length of each single NSM laminate intercepted by a 45° shear crack, expressed as,

$$L_i = \begin{cases} \frac{s}{\cos \alpha + \sin \alpha} & i \leq l_{0.004} & i = 1 \dots \frac{n}{2} \\ \ell_{net} - \frac{s}{\cos \alpha + \sin \alpha} & i \leq l_{0.004} & i = \frac{n}{2} + 1 \dots n \end{cases} \quad (8)$$

where, α is the slope of the FRP bar with respect to the longitudinal axis of the beam; s is the horizontal FRP bar spacing; and ℓ_{net} , defined as follows:

$$\ell_{net} = \ell_b - \frac{2c}{\sin \alpha} \quad (9)$$

where, ℓ_b is the actual length of a FRP bar and c is the clear concrete cover of the internal longitudinal reinforcement.

The first limitation in Equation (3), $s.i/(\cos \alpha + \sin \alpha)$ and $\ell_{net} - s.i/(\cos \alpha + \sin \alpha)$, takes into account bond as the controlling failure mechanism, and represents the minimum effective length of a FRP bar intercepted by a shear crack as a function of the term n :

$$n = \frac{\ell_{eff}(1 + \cot \alpha)}{s} \quad (10)$$

where, n is rounded off to the lowest integer (e.g., $n = 10.7 \Rightarrow n = 10$), and ℓ_{eff} represents the vertical length of ℓ_{net} , as follows:

$$\ell_{eff} = \ell_b \sin \alpha - 2c \quad (11)$$

The second limitation in Equation (3), $l_{0.004}$, considers the shear integrity of the concrete by limiting at 0.004 the maximum strain in the FRP reinforcement. From the force equilibrium condition and for rectangular bars, $l_{0.004}$ can be determined as follows:

$$l_{0.004} = 0.002 \frac{a \cdot b}{a + b} \frac{E_f}{\tau_b} \quad (12)$$

where, E_f represents the elastic modulus of the FRP bar.

The analytical values (V_t^{ana}), and the corresponding k values are provided in Table 5. Figure 9 also shows a comparison between V_t^{ana} and V_t^{exp} .

It is noteworthy that for beam FD-45, there were no CFRP laminates have been intercepted by the shear cracks; therefore, L_i (Equation (8)) is 0, so L_{tot} is 0, and consequently, the value of V_f (Equation (7)) is 0. However, V_t^{ana} is not 0 as there are values for V_c and V_s . However, as the value of V_t^{ana} for this beam is far from the values of other beams, it is excluded from the calculation of k and not considered in Figure 9.

The average k value was 0.73 with a corresponding value of standard deviation value of 0.125. It was noticed that all specimens have k values below the unity, as shown in Table 5. Figure 9 also shows that all beams are in the unsafe zone (below the diagonal line). This indicates that the formula proposed by Nanni et al.²⁹ could not provide satisfactory values of V_f and could not be conservatively used in the shear design of the NSM-FRP-strengthened RC beams in this study.

5 | CONCLUSIONS

The effects of length and inclination of NSM-CFRP laminates on the shear behavior of RC beams have been investigated in this study. The following points summarize the main findings and conclusions of this study.

- NSM-CFRP strengthening increased the load-carrying capacity, ductility, stiffness, and toughness from 8% to 41%, 9% to 78%, 24% to 159%, and 22% to 254%, respectively.
- As the CFRP laminate length decreases, the efficiency of the strengthening process increases. This is because the crack faces a non-grooved surface which could delay its formation somewhat.
- It can be concluded that changing the CFRP length had a greater effect on the maximum loads and deflections than varying the inclination angles, except in the case of the beam strengthened with 5 cm-trimmed laminates (T₅-45). This may confirm that using shorter CFRP laminates may result in a more effective strengthening process.
- The specimens strengthened with inclined CFRP laminates showed more increment in terms of load-carrying capacity, maximum deflection, stiffness, and toughness than those strengthened with vertical strips.
- Almost all the specimens failed in shear leading to concrete crushing, which resulted in the peeling-off of the side concrete cover and delamination of the bottom cover. This meant that the strengthening process could

not completely prevent shear crack formation, but it could delay their propagation and, thereby, failure.

- No debonding failure or fracture of FRP strips occurred, which are very common in the case of the EBR-FRP strengthening system.
- The analytical values of V_f obtained from the formula proposed by Dias and Barros⁴ has shown an unagreement with the experimental values, as the majority of specimens' safety factor (k) values were less than the unity, which indicates that these beams are in the unsafe zone. The average value of k was 0.80, and the corresponding standard deviation value was 0.195. The formula proposed by Nanni et al.²⁹ has also exhibited unsatisfactory results, where all the beams lay in the unsafe zone. The average value of k was 0.73, and the corresponding standard deviation value was 0.125.
- The formula proposed by Dias and Barros⁴ provided a higher average value of k and a higher value of standard deviation compared with those obtained when using the formula proposed by Nanni et al.²⁹. That indicates that the former offers better performance but less accurate results regarding the shear design of NSM-FRP-strengthened beams.
- The groove construction (dimensions) considered in this study was taken according to ACI 440.2 R-08,²⁸ and the same groove dimensions were considered for all strengthened specimens, so its effect on the beam capacity was not investigated in this study.
- It was confirmed that the groove size plays a key role in the performance of the NSM-FRP-strengthened concrete elements, in terms of the load-carrying capacity and the corresponding bond strength between FRP materials and concrete substrate.
- Further research studies to investigate the effect of bonded length of NSM-CFRP laminates on the performance of shear-strengthened RC beams are needed.

ACKNOWLEDGMENT

The authors wish to acknowledge the assistance of the technicians at the JUST Civil Engineering laboratories. This work was supported by the Deanship of Research at Jordan University of Science and Technology, via research grant number (214/2016).

DATA AVAILABILITY STATEMENT


The data that support the findings of this study are available from the corresponding author upon reasonable request.

ORCID

Mizi Fan  <https://orcid.org/0000-0002-6609-3110>

Yousef Al Rjoub  <https://orcid.org/0000-0003-3833-3495>

Ahmed Ashteyat  <https://orcid.org/0000-0002-8833-5133>

Mazen J. Al-Kheetan  <https://orcid.org/0000-0001-8366-7932>

REFERENCES

1. Al-Saadi NTK, Mohammed A, Al-Mahaidi R, Sanjayan J. A state-of-the-art review: near-surface mounted FRP composites for reinforced concrete structures. *Construct Build Mater.* 2019; 209:748–69.
2. Bakis CE, Bank LC, Brown V, Cosenza E, Davalos JF, Lesko JJ, et al. Fiber-reinforced polymer composites for construction—state-of-the-art review. *J Compos Constr.* 2002;6(2):73–87.
3. Dias SJE, Barros JAO. Shear strengthening of RC T-section beams with low strength concrete using NSM CFRP laminates. *Cem Concr Compos.* 2011;33(2):334–45.
4. Dias SJ, Barros JA. Shear strengthening of RC beams with NSM CFRP laminates: experimental research and analytical formulation. *Compos Struct.* 2013;99:477–90.
5. Dias SJ, Barros JA. NSM shear strengthening technique with CFRP laminates applied in high T cross section RC beams. *Compos Part B Eng.* 2017;114:256–67.
6. Oehlers D, Seracino R. Design of FRP and steel plated RC structures: retrofitting beams and slabs for strength, stiffness, and ductility. Oxford, England: Elsevier; 2004.
7. Oehlers DJ, Ju G, Liu IST, Seracino R. Moment redistribution in continuous plated RC flexural members. Part 1: neutral axis depth approach and tests. *Eng Struct.* 2004;26(14):2197–207.
8. Seracino R, Jones NM, Ali MS, Page MW, Oehlers DJ. Bond strength of near-surface mounted FRP strip-to-concrete joints. *J Compos Constr.* 2007;11(4):401–9.
9. Liu IS, Oehlers DJ, Seracino R. Tests on the ductility of reinforced concrete beams retrofitted with FRP and steel near-surface mounted plates. *J Compos Constr.* 2006;10(2):106–14.
10. Mukhopadhyaya P, Swamy N. Interface shear stress: a new design criterion for plate debonding. *J Compos Constr.* 2001;5(1):35–43.
11. Nguyen DM, Chan TK, Cheong HK. Brittle failure and bond development length of CFRP-concrete beams. *J Compos Constr.* 2001;5(1):12–7.
12. Asplund SO. Strengthening bridge slabs with grouted reinforcement. *J Proc.* 1949;45(1):397–406.
13. Dias SJ, Barros JA. Performance of reinforced concrete T beams strengthened in shear with NSM CFRP laminates. *Eng Struct.* 2010;32(2):373–84.
14. Rizzo A, De Lorenzis L. Behavior and capacity of RC beams strengthened in shear with NSM FRP reinforcement. *Construct Build Mater.* 2009;23(4):1555–67.
15. Al-Mahmoud F, Castel A, Minh TQ, François R. Reinforced concrete beams strengthened with NSM CFRP rods in shear. *Adv Struct Eng.* 2015;18(10):1563–74.
16. Sun W, Lou T, Achintha M. A novel strong and durable near-surface mounted (NSM) FRP method with cost-effective fillers. *Compos Struct.* 2021;255:112952.
17. Dias SJ and Barros JA. Behaviour of RC Beams Shear Strengthening with NSM CFRP Laminates. Porto: Universidade do Porto; 2008.
18. Dias SJ and Barros JA. Shear Strengthening of RC Beams with Near-Surface-Mounted CFRP Laminates. American Concrete Institute. Kansas City, MO: American Concrete Institute; 2005.
19. Barros JA, Dias SJ. Near surface mounted CFRP laminates for shear strengthening of concrete beams. *Cem Concr Compos.* 2006;28(3):276–92.
20. Dias SJ, Barros JA. Experimental behaviour of RC beams shear strengthened with NSM CFRP laminates. *Strain.* 2012;48(1):88–100.
21. De Lorenzis L, Nanni A. Shear strengthening of reinforced concrete beams with near-surface mounted fiber-reinforced polymer rods. *Struct J.* 2001a;98(1):60–8.
22. Dias SJ, Barros JA. Influence of the percentage of steel stirrups in the effectiveness of the NSM laminates shear strengthening technique. In FRPRCS-9, 9th International Symposium on Fiber Reinforced Polymer Reinforcement for Concrete Structures; 2009.
23. Mofidi A, Chaallal O, Cheng L, Shao Y. Investigation of near surface-mounted method for shear rehabilitation of reinforced concrete beams using fiber reinforced-polymer composites. *J Compos Constr.* 2016;20(2):04015048.
24. Tanarlan HM. The effects of NSM CFRP reinforcements for improving the shear capacity of RC beams. *Construct Build Mater.* 2011;25(5):2663–73.
25. Parretti R, Nanni A. Strengthening of RC members using near-surface mounted FRP composites: design overview. *Adv Struct Eng.* 2004;7(6):469–83.
26. Islam AA. Effects of NSM CFRP bars in shear strengthening of concrete members. Structures Congress 2009: Don't Mess With Structural Engineers: Expanding Our Role; Austin, TX: ASCE; 2009. p. 1–14.
27. ACI Committee. Building Code Requirements for Structural Concrete (ACI 318-05) and Commentary (ACI 318R-05). American Concrete Institute. Farmington Hills, MI: American Concrete Institute; 2005.
28. American Concrete Institute. Committee 440, 2008. Guide for the Design and Construction of Externally Bonded FRP Systems for Strengthening Concrete Structures: ACI 440.2 R-08. Farmington Hills, MI: American Concrete Institute; 2008.
29. Nanni A, Ludovico MD, Parretti R. Shear strengthening of a PC bridge girder with NSM CFRP rectangular bars. *Adv Struct Eng.* 2004;7(4):297–309.
30. Khalifa A, Gold WJ, Nanni A, MI AA. Contribution of externally bonded FRP to shear capacity of RC flexural members. *J Compos Constr.* 1998;2(4):195–202.
31. ACI Committee. Guide for the Design and Construction of Externally Bonded FRP Systems for Strengthening Concrete Structures (ACI 440.2R-02). Farmington Hills, MI: American Concrete Institute; 2002.
32. Hassan T, Rizkalla S. Investigation of bond in concrete structures strengthened with near surface mounted carbon fiber reinforced polymer strips. *J Compos Constr.* 2003;7(3):248–57.
33. Hassan T, Rizkalla S. Bond mechanism of NSM FRP bars for flexural strengthening of concrete structures. *ACI Struct J.* 2004;101(6):830–9.
34. De Lorenzis L, Nanni A. Bond between near-surface mounted fiber-reinforced polymer rods and concrete in structural strengthening. *Struct J.* 2002;99(2):123–32.
35. Galati D, De Lorenzis L. Effect of construction details on the bond performance of NSM FRP bars in concrete. *Adv Struct Eng.* 2009;12(5):683–700.
36. Novidis D, Pantazopoulou SJ, Tentolouris E. Experimental study of bond of NSM-FRP reinforcement. *Construct Build Mater.* 2007;21(8):1760–70.
37. Lorenzis LD, Nanni A. Characterization of FRP rods as near-surface mounted reinforcement. *J Compos Constr.* 2001b;5(2): 114–21.
38. Sharaky IA, Torres L, Baena M, Miàs C. An experimental study of different factors affecting the bond of NSM FRP bars in concrete. *Compos Struct.* 2013;99:350–65.

39. Soliman SM, El-Salakawy E, Benmokrane B. Bond performance of near-surface-mounted FRP bars. *J Compos Constr.* 2011;15(1):103–11.
40. Gómez J, Torres L, Barris C. Characterization and simulation of the bond response of NSM FRP reinforcement in concrete. *Materials.* 2020;13(7):1770.
41. Al-Mahmoud F, Castel A, François R, Tourneur C. Anchorage and tension-stiffening effect between near-surface-mounted CFRP rods and concrete. *Cem Concr Compos.* 2011;33(2):346–52.

AUTHOR BIOGRAPHIES



Mazen J. Al-Kheetan

Civil and Environmental Engineering Department,
College of Engineering, Mutah University,
Mutah, Karak 61710, Jordan, P.O. BOX 7.
mazen.al-kheetan@mutah.edu.jo



Mizi Fan

Department of Civil and Environmental Engineering,
College of Engineering, Design and Physical Sciences
Brunel University London, Kingston Ln,
Uxbridge, Middlesex, United Kingdom, UB8 3PH
mizi.fan@brunel.ac.uk



Yousef Al Rjoub

Civil Engineering Department,
College of Engineering,
Jordan University of Science and Technology,
Irbid 22110, P.O. Box 3030, Jordan
ysalrjoub@just.edu.jo



Ahmed Ashteyat

Civil Engineering Department,
College of Engineering,
The University of Jordan,
Amman 11942, Jordan
a.ashteyat@ju.edu.jo



Mohammad Al-Zu'bi

Department of Civil and Environmental Engineering,
College of Engineering, Design and Physical Sciences,
Brunel University London, Kingston Ln,
Uxbridge, Middlesex, United Kingdom, UB8 3PH
mohammadibrahimawad.al-zu'bi@brunel.ac.uk



Lorna Anguilano

Experimental Techniques Centre,
College of Engineering, Design and Physical Sciences,
Brunel University London,
Uxbridge, Middlesex, United Kingdom, UB8 3PH
lorna.anguilano@brunel.ac.uk

How to cite this article: Al-Zu'bi M, Fan M, Al Rjoub Y, Ashteyat A, Al-Kheetan MJ, Anguilano L. The effect of length and inclination of carbon fiber reinforced polymer laminates on shear capacity of near-surface mounted retrofitted reinforced concrete beams. *Structural Concrete.* 2021;1–15.
<https://doi.org/10.1002/suco.202100198>